

# Resampling the Ensemble Kalman Filter

I. Myrseth<sup>a,\*</sup>, J. Sætrum<sup>b</sup>, H. Omre<sup>c</sup>

<sup>a</sup>*Norwegian Computing Center, Gaustadalleen 23b, NO-0314 Oslo, Norway*

<sup>b</sup>*Statoil ASA, Vestre Svanholmen 1, NO-4033 Stavanger, Norway*

<sup>c</sup>*Norwegian University of Science and Technology, NO-7491 Trondheim, Norway*

---

## Abstract

Ensemble Kalman filters (EnKF) based on a small ensemble tend to provide collapse of the ensemble over time. It is demonstrated that this collapse is caused by positive coupling of the ensemble members due to use of the estimated Kalman gain for the update of all ensemble members at each time step. This coupling can be avoided by resampling the Kalman gain from its sampling distribution in the conditioning step. In the analytically tractable Gauss-linear model finite sample distributions for all covariance matrix estimates involved in the Kalman gain estimate are known and hence exact Kalman gain resampling can be done. For the general nonlinear case we introduce the resampling ensemble Kalman filter (ResEnKF) algorithm. The resampling strategy in the algorithm is based on bootstrapping of the ensemble and Monte Carlo simulation of the likelihood model. We also define a semi-parametric and parametric version of the resampling ensemble Kalman filter algorithm. An empirical study demonstrates that ResEnKF provides more reliable prediction intervals than traditional EnKF, on the cost of somewhat less accuracy in the point predictions.

---

\*Corresponding author. email:myrseth@nr.no, tel:+4722852697

*Keywords:* Ensemble Kalman filter, Kalman gain sampling, Monte Carlo, Bootstrap

---

## 1. Introduction

The Ensemble Kalman Filter (EnKF) introduced by Evensen in the papers Evensen (1994) and Burgers et al. (1998) has found widespread use in evaluation of spatio-temporal phenomena like ocean modeling, weather forecasting and petroleum reservoir evaluation, see Bertino et al. (2002), Houtekamer et al. (2005), Nævdal et al. (2005) and references therein. The filter is popular because of easy implementation and computational efficiency. The filter relies on simulation based inference of hidden Markov models and is closely related to the traditional Kalman filter. The EnKF utilizes a linearization in the data conditioning and relies on empirical probability densities, represented as an ensemble of possible states, which allow general forward functions. These approximations make the ensemble Kalman filter computationally efficient and well suited for high-dimensional hidden Markov models.

The data conditioning is based on the estimated correlation between observations and ensemble members, which is used to update all ensemble members. The estimated regression weights, so called Kalman gain in the case with linear observation relations, is associated with finite sample uncertainty usually resulting in underestimated Kalman gain, see Furrer & Bengtsson (2007). Anderson (2001) deals with the problem by variance inflation in an effort to maintain variability in the ensemble statistics. One of the key assumptions in the data conditioning is that the ensemble members are inde-

23 pendent. However, when using the estimated Kalman gain to update every  
24 ensemble member, the ensemble members will be coupled over time.

25 In the hierarchical ensemble Kalman filter (HEnKF) algorithm (Myrseth  
26 & Omre, 2010) uncertainty caused by the Kalman gain estimate is accounted  
27 for. The HEnKF algorithm relies on an extended model of the prior on the  
28 model parameters, however. Houtekamer & Mitchell (1998) use a double  
29 ensemble approach where one part of the ensemble is used in the estimation  
30 of the Kalman gain used in the update step of the other part. However, this  
31 ensures that the ensemble members are uncoupled after the first update step  
32 only. In the current paper, we propose to update every ensemble member  
33 individually with different estimates of the Kalman gain using a bootstrap-  
34 ping technique (Efron, 1979). The estimation uncertainty associated with  
35 the Kalman gain will then be reflected in the ensemble uncertainty. We  
36 also introduce formalism that handles non-linear relations between state and  
37 observation.

## 38 2. Model Assumptions

39 Consider an unknown, multivariate time series  $[\mathbf{x}_0, \mathbf{x}_1, \dots, \mathbf{x}_T, \mathbf{x}_{T+1}]$  with  
40  $\mathbf{x}_t \in \mathbb{R}^{p_x}$ ;  $t = 0, \dots, T + 1$  containing the primary variable of interest and  $\mathbf{x}_T$   
41 being the current state. Assume that an associated time series of observations  
42  $[\mathbf{d}_0, \dots, \mathbf{d}_T]$  with  $\mathbf{d}_t \in \mathbb{R}^{p_d}$ ;  $t = 0, \dots, T$ , is available.

43 Define a prior stochastic model for  $[\mathbf{x}_0, \dots, \mathbf{x}_{T+1}]$  by assuming Markov

44 properties:

$$\begin{aligned}
[\mathbf{x}_0, \dots, \mathbf{x}_{T+1}] &\sim f(\mathbf{x}_0, \dots, \mathbf{x}_{T+1}) \\
&= f(\mathbf{x}_0) \prod_{t=0}^T f(\mathbf{x}_{t+1} | \mathbf{x}_0, \dots, \mathbf{x}_t) \\
&= f(\mathbf{x}_0) \prod_{t=0}^T f(\mathbf{x}_{t+1} | \mathbf{x}_t). \tag{1}
\end{aligned}$$

45 Let  $f(\mathbf{x}_0)$  be a known pdf for the initial state, and  $f(\mathbf{x}_{t+1} | \mathbf{x}_t)$  for  $t = 0, \dots, T$   
46 be known forward pdfs. Hence the prior model for the time series of interest  
47 is Markovian with each state given the past, dependent on the previous state  
48 only.

49 Define the likelihood model for  $[\mathbf{d}_0, \dots, \mathbf{d}_T]$  given  $[\mathbf{x}_0, \dots, \mathbf{x}_{T+1}]$  by assuming  
50 conditional independence and single state dependence:

$$\begin{aligned}
[\mathbf{d}_0, \dots, \mathbf{d}_T | \mathbf{x}_0, \dots, \mathbf{x}_{T+1}] &\sim f(\mathbf{d}_0, \dots, \mathbf{d}_T | \mathbf{x}_0, \dots, \mathbf{x}_{T+1}) \\
&= \prod_{t=0}^T f(\mathbf{d}_t | \mathbf{x}_0, \dots, \mathbf{x}_{t+1}) \\
&= \prod_{t=0}^T f(\mathbf{d}_t | \mathbf{x}_t) \tag{2}
\end{aligned}$$

51 where  $f(\mathbf{d}_t | \mathbf{x}_t)$  for  $t = 0, \dots, T$  are known likelihood functions. Hence, the  
52 likelihood model entails that the observation at time  $t$  is a function of state  
53  $\mathbf{x}_t$  only and is independent of the other observations when  $\mathbf{x}_t$  is given.

54 These prior and likelihood assumptions define a hidden Markov process  
55 as depicted by the graph in Figure 1. The resulting posterior stochastic

56 model is defined by Bayesian inversion:

$$\begin{aligned}
[\mathbf{x}_0, \dots, \mathbf{x}_{T+1} | \mathbf{d}_0, \dots, \mathbf{d}_T] &\sim f(\mathbf{x}_0, \dots, \mathbf{x}_{T+1} | \mathbf{d}_0, \dots, \mathbf{d}_T) \\
&= \text{const} \times f(\mathbf{d}_0, \dots, \mathbf{d}_T | \mathbf{x}_0, \dots, \mathbf{x}_{T+1}) \\
&\quad \times f(\mathbf{x}_0, \dots, \mathbf{x}_{T+1}) \\
&= \text{const} \times f(\mathbf{x}_0) f(\mathbf{d}_0 | \mathbf{x}_0) \\
&\quad \times \left[ \prod_{t=0}^{T-1} f(\mathbf{d}_{t+1} | \mathbf{x}_{t+1}) f(\mathbf{x}_{t+1} | \mathbf{x}_t) \right] \\
&\quad \times f(\mathbf{x}_{T+1} | \mathbf{x}_T), \tag{3}
\end{aligned}$$

57 with ‘const’ being a normalizing constant that is usually hard to assess.

58 Hence the full posterior model is not easily available.

59 For the hidden Markov model described, the forecast is of interest. The  
60 forecasting pdf is available as:

$$\begin{aligned}
[\mathbf{x}_{T+1} | \mathbf{d}_0, \dots, \mathbf{d}_T] &\sim f(\mathbf{x}_{T+1} | \mathbf{d}_0, \dots, \mathbf{d}_T) \\
&= \int \dots \int f(\mathbf{x}_0, \dots, \mathbf{x}_{T+1} | \mathbf{d}_0, \dots, \mathbf{d}_T) d\mathbf{x}_0 \dots d\mathbf{x}_T. \tag{4}
\end{aligned}$$

61 This forecasting pdf is computable by a recursive algorithm which alternates  
62 a forward-in-time step and a condition-on-data step. This recursive algorithm  
63 makes sequential conditioning on future observations possible.

64 The model described above can be summarized by the following general  
65 state space equations:

$$\begin{aligned}
\mathbf{x}_0 &\sim f(\mathbf{x}_0) \\
\mathbf{x}_{t+1} | \mathbf{x}_t &= \omega_t(\mathbf{x}_t, \boldsymbol{\epsilon}_t^{\mathbf{x}}) \sim f(\mathbf{x}_{t+1} | \mathbf{x}_t) \\
\mathbf{d}_t | \mathbf{x}_t &= \nu_t(\mathbf{x}_t, \boldsymbol{\epsilon}_t^{\mathbf{d}}) \sim f(\mathbf{d}_t | \mathbf{x}_t), \tag{5}
\end{aligned}$$

66 where  $\omega_t(\cdot, \cdot)$  is a known function  $\mathbb{R}^{2p_x} \rightarrow \mathbb{R}^{p_x}$  and  $\boldsymbol{\epsilon}_t^x$  is a random vari-  
67 able from the normalized  $p_x$ -dimensional multivariate Gaussian distribution  
68  $N_{p_x}(\mathbf{0}, \mathbf{I}_{p_x})$  where  $\mathbf{I}_{p_x}$  is a unit diagonal covariance matrix,  $\nu_t(\cdot, \cdot)$  is a known  
69 function  $\mathbb{R}^{p_x+p_d} \rightarrow \mathbb{R}^{p_d}$  and  $\boldsymbol{\epsilon}_t^d$  is a normalized  $p_d$ -dimensional Gaussian ran-  
70 dom variable from  $N_{p_d}(\mathbf{0}, \mathbf{I}_{p_d})$ . This construction can generate a realization  
71 from an arbitrary forward,  $f(\mathbf{x}_{t+1}|\mathbf{x}_t)$ , and likelihood,  $f(\mathbf{d}_t|\mathbf{x}_t)$ , model.

### 72 3. The Ensemble Kalman Filter

73 The EnKF is an algorithm that can be used to assess the forecasting  
74 pdf. The basic idea of the EnKF to represent an empirical distribution  
75 approximating the true prior by a set of realizations, so called ensemble.  
76 These realizations are adjusted according to the likelihood model when an  
77 observation occurs and the adjusted realizations are then taken through the  
78 forward model to the next observation time. At time  $t = T + 1$  a set of  
79 approximately independent realizations are available for empirical assessment  
80 of  $f(\mathbf{x}_{T+1}|\mathbf{d}_0, \dots, \mathbf{d}_T)$ . Hence, characteristics beyond the two first moments  
81 can be captured. Basic references for EnKF are Evensen (1994), Burgers  
82 et al. (1998), Evensen (2007) and references therein.

83 Introduce the following notation, with

$$\begin{aligned} \mathbf{x}_t^u &= [\mathbf{x}_t | \mathbf{d}_0, \dots, \mathbf{d}_{t-1}] \\ \mathbf{x}_t^c &= [\mathbf{x}_t | \mathbf{d}_0, \dots, \mathbf{d}_t], \end{aligned} \quad (6)$$

where indices  $u$  and  $c$  indicate unconditioned and conditioned on the obser-  
vation at the current time, respectively. Define a time series of ensembles:

$$\mathbf{e}_t : \{(\mathbf{x}_t^u, \mathbf{d}_t)^{(i)}; i = 1, \dots, n_e\}; t = 0, \dots, T + 1, \quad (7)$$

where  $\mathbf{x}_t^{u(i)} = [\mathbf{x}_t | \mathbf{d}_0, \dots, \mathbf{d}_{t-1}]^{(i)}$  are approximate realizations from  $f(\mathbf{x}_t | \mathbf{d}_0, \dots, \mathbf{d}_{t-1})$  and  $[\mathbf{d}_t^{(i)} | \mathbf{x}_t^{u(i)}] = \nu(\mathbf{x}_t^{u(i)}, \boldsymbol{\epsilon}_t^{\mathbf{d}(i)})$  are associated realizations of the observation available at time  $t$ . Note that at any step  $t$  - with  $t$  omitted in the notation - one has the expectation vector and covariance matrix:

$$\boldsymbol{\mu}_{\mathbf{xd}} = \begin{bmatrix} \mathbb{E}\{\mathbf{x}^u\} \\ \mathbb{E}\{\mathbf{d}\} \end{bmatrix} = \begin{bmatrix} \boldsymbol{\mu}_{\mathbf{x}} \\ \boldsymbol{\mu}_{\mathbf{d}} \end{bmatrix} \quad (8)$$

and

$$\boldsymbol{\Sigma}_{\mathbf{xd}} = \begin{bmatrix} \text{Cov}\{\mathbf{x}^u\} & \text{Cov}\{\mathbf{x}^u, \mathbf{d}\} \\ \text{Cov}\{\mathbf{d}, \mathbf{x}^u\} & \text{Cov}\{\mathbf{d}\} \end{bmatrix} = \begin{bmatrix} \boldsymbol{\Sigma}_{\mathbf{x}} & \boldsymbol{\Gamma}_{\mathbf{x},\mathbf{d}} \\ \boldsymbol{\Gamma}_{\mathbf{d},\mathbf{x}} & \boldsymbol{\Sigma}_{\mathbf{d}} \end{bmatrix}. \quad (9)$$

The traditional EnKF, see Evensen (2007), is defined with a Gauss-linear likelihood model

$$\mathbf{d}_t | \mathbf{x}_t = H_t \mathbf{x}_t + \boldsymbol{\epsilon}_t, \quad (10)$$

84 with  $\boldsymbol{\epsilon}_t$  being  $N_{p_{\mathbf{d}}}(\mathbf{0}, \boldsymbol{\Sigma}_{\mathbf{d}|\mathbf{x}})$ , or a linearization of a nonlinear likelihood model.

85 The associated traditional EnKF algorithm is presented in Algorithm 1.

86 The EnKF algorithm is recursive and each recursion consists of a condi-  
87 tioning operation and a forwarding operation. The conditioning expression is  
88 linear with weights estimated from the ensemble. The forwarding operation  
89 is defined by the forward pdf. This entails two implicit approximations in  
90 the EnKF:

91 The sample space of  $\mathbf{x}_t$  is discretized and represented by a finite number of  
92 realizations. Initially an ensemble of iid realizations is assumed to represent  
93  $f(\mathbf{x}_0)$ . For high-dimensional problems a large number of ensemble members  
94 may be required to do so reliably.

95 The data conditioning expression is linearized. Moreover, the weights

---

**Algorithm 1:** Traditional Ensemble Kalman filter
 

---

Initiate:

- $n_e$  = no. of ensemble members
- $\mathbf{x}_0^{u(i)}$ ;  $i = 1, \dots, n_e$  iid  $f(\mathbf{x}_0)$
- $\boldsymbol{\epsilon}_0^{\mathbf{d}(i)} \sim N_{p_d}(\mathbf{0}, \Sigma_{\mathbf{d}|\mathbf{x}})$ ;  $i = 1, \dots, n_e$
- $\mathbf{d}_0^{(i)} = H_0 \mathbf{x}_0^{u(i)} + \boldsymbol{\epsilon}_0^{\mathbf{d}(i)}$ ;  $i = 1, \dots, n_e$
- $\mathbf{e}_0 : \{(\mathbf{x}_0^u, \mathbf{d}_0)^{(i)}; i = 1, \dots, n_e\}$

 for  $t = 0$  to  $T$  do

Conditioning:

- Estimate  $\widehat{\Sigma}_{\mathbf{x}}$  from  $\mathbf{e}_t$
- $\widehat{\Gamma}_{\mathbf{x}, \mathbf{d}} = \widehat{\Sigma}_{\mathbf{x}} H_t'$
- $\widehat{\Sigma}_{\mathbf{d}} = H_t \widehat{\Sigma}_{\mathbf{x}} H_t' + \Sigma_{\mathbf{d}|\mathbf{x}}$
- $\mathbf{x}_t^{c(i)} = \mathbf{x}_t^{u(i)} + \widehat{\Gamma}_{\mathbf{x}, \mathbf{d}} \widehat{\Sigma}_{\mathbf{d}}^{-1} (\mathbf{d}_t - \mathbf{d}_t^{(i)})$ ;  $i = 1, \dots, n_e$

Forwarding:

- $\boldsymbol{\epsilon}_t^{\mathbf{x}(i)} \sim N_{p_x}(\mathbf{0}, \mathbf{I}_{p_x})$ ;  $i = 1, \dots, n_e$
- $\mathbf{x}_{t+1}^{u(i)} = \omega_t(\mathbf{x}_t^{c(i)}, \boldsymbol{\epsilon}_t^{\mathbf{x}(i)})$ ;  $i = 1, \dots, n_e$
- $\boldsymbol{\epsilon}_{t+1}^{\mathbf{d}(i)} \sim N_{p_d}(\mathbf{0}, \Sigma_{\mathbf{d}|\mathbf{x}})$ ;  $i = 1, \dots, n_e$
- $\mathbf{d}_{t+1}^{(i)} = H_{t+1} \mathbf{x}_{t+1}^{u(i)} + \boldsymbol{\epsilon}_{t+1}^{\mathbf{d}(i)}$ ;  $i = 1, \dots, n_e$
- $\mathbf{e}_{t+1} : \{(\mathbf{x}_{t+1}^u, \mathbf{d}_{t+1})^{(i)}; i = 1, \dots, n_e\}$

Assess

- $f(\mathbf{x}_{T+1} | \mathbf{d}_0, \dots, \mathbf{d}_T)$  from  $\mathbf{e}_{T+1}$
-



96 in the linearization are estimated from the ensemble. Note, however, that  
 97 each ensemble member is conditioned individually and hence the lineariza-  
 98 tion only applies to the conditioning not to the forward model. For highly  
 99 non-Gaussian prior models and/or strongly nonlinear likelihood models this  
 100 approximation may provide unreliable results.

101 Under these approximations, however, all types of models for the hidden  
 102 Markov process can be evaluated. Other problems arise in the EnKF which  
 103 are caused by the use of an estimate of the Kalman gain based on  $\mathbf{e}_t$  instead  
 104 of the true weights. These problems include rank deficiency and estimation  
 105 uncertainty due to the limited size of the ensemble, i.e., small values of  $n_{\mathbf{e}}$ .  
 106 A discussion of the implications of data conditioning based on finite sample  
 107 ensemble statistics follows.

### 108 3.1. The conditioning step

The conditioning step in the EnKF contains the linear approximation that appears crucial for the success of the filter. The conditioning expression relies on the Kalman gain  $K = \Gamma_{\mathbf{x},\mathbf{d}}\Sigma_{\mathbf{d}}^{-1}$ , which must be estimated at each state from the  $n_{\mathbf{e}}$  members of the ensemble  $\mathbf{e}_t$ . In the general case with nonlinear likelihood model, the classical covariance estimators are applied:

$$\hat{\Gamma}_{\mathbf{x},\mathbf{d}} = \frac{1}{n_{\mathbf{e}} - 1} \sum_{i=1}^{n_{\mathbf{e}}} (\mathbf{x}_t^{u(i)} - \hat{\boldsymbol{\mu}}_{\mathbf{x}})(\mathbf{d}_t^{(i)} - \hat{\boldsymbol{\mu}}_{\mathbf{d}})' \quad (11)$$

$$\hat{\Sigma}_{\mathbf{d}} = \frac{1}{n_{\mathbf{e}} - 1} \sum_{i=1}^{n_{\mathbf{e}}} (\mathbf{d}_t^{(i)} - \hat{\boldsymbol{\mu}}_{\mathbf{d}})(\mathbf{d}_t^{(i)} - \hat{\boldsymbol{\mu}}_{\mathbf{d}})', \quad (12)$$

with

$$\hat{\boldsymbol{\mu}}_{\mathbf{x}} = \frac{1}{n_{\mathbf{e}}} \sum_{i=1}^{n_{\mathbf{e}}} \mathbf{x}_t^{u(i)} \quad (13)$$

and

$$\hat{\boldsymbol{\mu}}_{\mathbf{d}} = \frac{1}{n_{\mathbf{e}}} \sum_{i=1}^{n_{\mathbf{e}}} \mathbf{d}_t^{(i)}. \quad (14)$$

109 If  $\mathbf{e}_t$  contains independent members these estimators are unbiased and con-  
 110 sistent. The latter entails  $\hat{\Gamma}_{\mathbf{x},\mathbf{d}} \rightarrow \Gamma_{\mathbf{x},\mathbf{d}}$  and  $\hat{\Sigma}_{\mathbf{d}} \rightarrow \Sigma_{\mathbf{d}}$  as  $n_{\mathbf{e}} \rightarrow \infty$ , for all  
 111 distributional models. Moreover,  $\hat{K} = \hat{\Gamma}_{\mathbf{x},\mathbf{d}} \hat{\Sigma}_{\mathbf{d}}^{-1} \rightarrow K$  as  $n_{\mathbf{e}} \rightarrow \infty$ . Note that  
 112 in the traditional EnKF scheme defined in Algorithm 1,  $\hat{K}$  will be biased  
 113 estimate of  $K$ . The consequences of this bias are thoroughly discussed in  
 114 Furrer & Bengtsson (2007), where conditions on the size of  $n_{\mathbf{e}}$  for obtaining  
 115 bounded error growth is developed. It was recommended to use a boosting  
 116 or inflation factor to correct the variability for this bias. For finite  $n_{\mathbf{e}}$ , it  
 117 is known (Huber, 1981) that the classical estimators for covariance matrices  
 118 are notoriously unreliable due to extreme dependence on the tail behavior  
 119 of the underlying pdf. This sensitivity is caused by the second order terms  
 120 of the estimators. The lack of precision in  $\hat{K}$  may cause spurious values to  
 121 appear in the conditioned  $\mathbf{x}_t^c$ , which impact may be accelerated by non-linear  
 122 forward models.

The motivation for this study follows from a closer evaluation of the conditioning relation

$$\mathbf{x}^{c(i)} = \mathbf{x}^{u(i)} + \hat{K}(\mathbf{d} - \mathbf{d}^{(i)}); i = 1, \dots, n_{\mathbf{e}}, \quad (15)$$

where the time index is omitted for simplicity. Let the prior model for  $\mathbf{x}^u$  be a Gaussian and the likelihood be Gauss-linear with known model parameters. Then the Kalman gain

$$K = \Sigma_{\mathbf{x}} H' (H \Sigma_{\mathbf{x}} H' + \Sigma_{\mathbf{d}|\mathbf{x}})^{-1} \quad (16)$$

123 is known. For this case  $\mathbf{x}^c$  is Gaussian with  $E\{\mathbf{x}^c\} = E\{\mathbf{x}^u|\mathbf{d}\} = \mu_{\mathbf{x}|\mathbf{d}}$   
124 and  $\text{Cov}\{\mathbf{x}^c\} = \text{Cov}\{\mathbf{x}^u|\mathbf{d}\} = \Sigma_{\mathbf{x}|\mathbf{d}}$  which constitutes the correct solution  
125 when all model parameters are known. Moreover, if the ensemble members  
126  $\mathbf{x}_t^{u(i)}; i = 1, \dots, n_{\mathbf{e}}$  are independent, the resulting  $\mathbf{x}_t^{c(i)}; i = 1, \dots, n_{\mathbf{e}}$  will also  
127 be independent.

128 In practice, however, the model parameters are not known and the Kalman  
129 gain  $K$  must be estimated from the  $n_{\mathbf{e}}$  members of the ensemble  $\mathbf{e}$ . Since  
130 the conditioning will be based on an estimate of  $K$ , the resulting uncertainty  
131 in  $\mathbf{x}^c$  will be larger than if  $K$  was known. Assume that the elements in  
132  $\mathbf{e} : \{(\mathbf{x}^u, \mathbf{d})^{(i)}; i = 1, \dots, n_{\mathbf{e}}\}$  are independent and Gaussian and that  $n_{\mathbf{e}} > p_{\mathbf{x}}$ .  
133 Then the standard estimator of  $\Sigma_{\mathbf{x}}$  will be Wishart distributed, and estimates  
134 of  $\Sigma_{\mathbf{x}}$  can be simulated and by applying Expression (16) realizations of  $K$  can  
135 be generated. Hence  $K$  can be seen as a random variable  $K_{\mathbf{e}} \sim f(K_{\mathbf{e}})$ . In  
136 order to evaluate the characteristics of  $\mathbf{x}^c$  when  $K_{\mathbf{e}}$  is random, consider the  
137 Taylor expansion of Expression (15) around  $E\{K_{\mathbf{e}}\} = \mu_{K_{\mathbf{e}}}$  and  $E\{\mathbf{d}^{(i)}\} = \mu_{\mathbf{d}}$ :

$$\begin{aligned} \mathbf{x}^{c(i)} &\approx \mathbf{x}^{u(i)} + \mu_{K_{\mathbf{e}}}(\mathbf{d} - \mu_{\mathbf{d}}) - \mu_{K_{\mathbf{e}}}(\mathbf{d}^{(i)} - \mu_{\mathbf{d}}) \\ &\quad + (K_{\mathbf{e}} - \mu_{K_{\mathbf{e}}})(\mathbf{d} - \mu_{\mathbf{d}}) - (K_{\mathbf{e}} - \mu_{K_{\mathbf{e}}})(\mathbf{d}^{(i)} - \mu_{\mathbf{d}}) \\ &\quad ; i = 1, \dots, n_{\mathbf{e}} \end{aligned} \tag{17}$$

138  $K_{\mathbf{e}}$  is inferred from the complete set of ensemble members, hence the depen-  
139 dence between  $K_{\mathbf{e}}$  and each  $(\mathbf{x}^u, \mathbf{d})^{(i)}$  is relatively weak. In the expressions  
140 calculated below the two variables are assumed to be independent.

The following expressions can be developed from Expression (17)

$$\begin{aligned}
\mathbb{E}\{\mathbf{x}^{c(i)}\} &= \mu_{\mathbf{x}} + (\mu_{K_e} - K)(\mathbf{d} - \mu_{\mathbf{d}}) \\
\text{Cov}\{\mathbf{x}^{c(i)}\} &= \Sigma_{\mathbf{x}} + (\mu_{K_e} - K)\Sigma_{\mathbf{d}}(\mu_{K_e} - K)' \\
&\quad + \mathbb{E}\{(K_e - \mu_{K_e})(\Sigma_{\mathbf{d}} + \Delta_{\mathbf{d}})(K_e - \mu_{K_e})'\} \\
\text{Cov}\{\mathbf{x}^{c(i)}, \mathbf{x}^{c(j)}\} &= \mathbb{E}\{(K_e - \mu_{K_e})\Delta_{\mathbf{d}}(K_e - \mu_{K_e})'\} \tag{18}
\end{aligned}$$

141 for  $i, j = 1, \dots, n_e; i \neq j$ , where  $K$  is the true, but unknown Kalman weight  
142 and  $\Delta_{\mathbf{d}} = (\mathbf{d} - \mu_{\mathbf{d}})(\mathbf{d} - \mu_{\mathbf{d}})'$ . Hence, if  $K_e$  is an unbiased estimator for  $K$ , the  
143 conditioned ensemble members are correctly centered at  $\mu_{\mathbf{x}|\mathbf{d}}$ , while there is  
144 an additional  $K_e$  estimation term in the variance of the members. Note, that  
145 the cross ensemble covariance will be positive whenever there is estimation  
146 uncertainty in  $K_e$ . Hence the members of the conditioned ensemble will be  
147 positively coupled and the empirical covariance matrix based on the ensemble  
148 will underestimate the covariance. This is alarming since the EnKF is based  
149 on a sequential conditioning through time meaning that the coupling will  
150 grow increasingly stronger. Lastly, note that as  $n_e \rightarrow \infty$  the uncertainty in  
151  $K_e$  decreases and all problems disappear.

152 One possible solution to avoid this coupling problem is to perform Kalman  
153 gain resampling:

$$\begin{aligned}
K_e^{(1)}, \dots, K_e^{(n_e)} &\text{ iid } f(K_e) \\
\mathbf{x}^{c(i)} &= \mathbf{x}^{u(i)} + K_e^{(i)}(\mathbf{d} - \mathbf{d}^{(i)}); i = 1, \dots, n_e \tag{19}
\end{aligned}$$

154 Then  $\mathbb{E}\{\mathbf{x}^c\}$  and  $\text{Cov}\{\mathbf{x}^c\}$  will remain the same as for Expression (15), while  
155  $\text{Cov}\{\mathbf{x}^{c(i)}, \mathbf{x}^{c(j)}\} = 0$ , and hence the ensemble coupling disappears. The as-

156 sessment of  $f(K_e)$  remains a challenge of course.

For the complete Gauss-linear model, all finite sample distributions are known. In particular it is known that  $\mathbf{x}^{(i)} \sim N_{p_x}(\boldsymbol{\mu}_x, \Sigma_x)$  at each conditioning step. The following resampling is reasonable:

$$\begin{aligned}
& \mathbf{do} \ i = 1, \dots, n_e \\
& \quad \mathbf{x}_\cdot^{(1)}, \dots, \mathbf{x}_\cdot^{(n_e)} \text{ iid } N_{p_x}(\boldsymbol{\mu}_x, \Sigma_x) \\
& \quad \Sigma_x^{(i)} = \frac{1}{n_e - 1} \sum_{j=1}^{n_e} (\mathbf{x}_\cdot^{(j)} - \bar{\mathbf{x}}_\cdot) \\
& \quad K_e^{(i)} = \Sigma_x^{(i)} H' (H \Sigma_x^{(i)} H' + \Sigma_{\mathbf{d}|\mathbf{x}})^{-1} \\
& \quad \mathbf{x}^{c(i)} = \mathbf{x}^{u(i)} + K_e^{(i)} (\mathbf{d} - \mathbf{d}^{(i)}) \\
& \mathbf{end do}
\end{aligned} \tag{20}$$

157 The resampling EnKF approach specified in Expression (20) is primar-  
158 ily aimed at restoring the independence between the conditioned ensemble  
159 members, thus improving the reliability of the prediction intervals. The vari-  
160 ability in the estimated Kalman gains  $K_e$  will remain and spurious values  
161 in  $\mathbf{x}^c$  will still occur. The Hierarchical EnKF (HEnKF) approach, presented  
162 in Myrseth & Omre (2010) aims at combining a shrinkage estimator for  $K_e$   
163 which reduce spurious values and the resampling approach defined above.  
164 The empirical study in Myrseth & Omre (2010) provides very encouraging  
165 results, but HEnKF requires additional modeling which can be difficult in  
166 large problems. In the current paper we present an empirical resampling  
167 approach which requires no additional modeling assumptions.

168 **4. Resampling**

169 Resampling or simulating from a known pdf is called Monte Carlo sim-  
170 ulation, see Hammersley & Handscomb (1964). This is sometimes the most  
171 efficient way to determine the pdf of random variables that are nonlinear  
172 functions of random variables with known pdfs. Actually, this is exactly the  
173 goal of the EnKF. The bootstrap, formally introduced in Efron (1979), is a  
174 statistical method to assess parameter uncertainty. Here we will only give a  
175 short introduction to the bootstrap and Monte Carlo techniques, and refer  
176 the interested reader to Efron & Tibshirani (1993).

177 Consider a random variable with an associated cdf,  $\mathbf{x} \sim F(\mathbf{x})$ , and some  
178 interesting characteristic of the cdf,  $\xi = h(F(\mathbf{x}))$ . Examples of this charac-  
179 teristic are the expectation  $E\{\mathbf{x}\}$ , covariance  $Cov\{\mathbf{x}\}$ , quantiles  $Prob\{\mathbf{x} \leq c\}$   
180 for some arbitrary  $c$  etc. Assume that a set of realizations  $\mathbf{x}_1, \dots, \mathbf{x}_n$  iid  $F(\mathbf{x})$   
181 are available and define a finite sample estimator of  $\xi$ ,  $\hat{\xi}_n = h_n(\mathbf{x}_1, \dots, \mathbf{x}_n)$ ,  
182 such that  $h_n(\mathbf{x}_1, \dots, \mathbf{x}_n) \xrightarrow{n \rightarrow \infty} h(F(\mathbf{x}))$ . The objective is to obtain the cdf of  
183 the finite sample estimator  $\hat{\xi}_n$ ,  $F_n(\xi)$ . If  $F(\mathbf{x})$  is fully known, then assessment  
184 of  $F_n(\xi)$  can be done by Monte Carlo simulation as described in Algorithm 2.

---

**Algorithm 2:** Monte Carlo simulation

---

Initiate:

- $m =$  no. of Monte Carlo replicates

**for**  $i = 1$  to  $m$  **do**

    Generate:  $\mathbf{x}_1^*, \dots, \mathbf{x}_n^*$  iid  $F(\mathbf{x})$   
     $\hat{\xi}_n^{(i)} = h_n(\mathbf{x}_1^*, \dots, \mathbf{x}_n^*)$

Estimate:  $F_n(\xi)$  from  $\hat{\xi}_n^{(1)}, \dots, \hat{\xi}_n^{(m)} \rightarrow \hat{F}_n(\xi)$

---

185

---

**Algorithm 3:** Bootstrap

---

Initiate:

- $b =$  no. of bootstrap replicates
- $\hat{F}(\mathbf{x}) = \frac{1}{n} \sum_{i=1}^n I(\mathbf{x}_i < \mathbf{x})$

**for**  $i = 1$  to  $b$  **do**

- Generate:  $\mathbf{x}_1^*, \dots, \mathbf{x}_n^*$  iid  $\hat{F}(\mathbf{x})$
- $\hat{\xi}_n^{*(i)} = h_n(\mathbf{x}_1^*, \dots, \mathbf{x}_n^*)$

Estimate:  $F_n(\xi)$  from  $\hat{\xi}_n^{*(1)}, \dots, \hat{\xi}_n^{*(b)} \rightarrow \hat{F}_n^*(\xi)$ 

---

186 The approximation depends on the number of Monte Carlo samples, and  
187 the finite sample pdf can be fully determined when the number of Monte  
188 Carlo samples tends to infinity,  $\hat{F}_n(\xi) \xrightarrow{m \rightarrow \infty} F_n(\xi)$ .

189 If  $F(\mathbf{x})$  is unknown, however, Monte Carlo assessment is unavailable and  
190 one may rely on the bootstrap technique. Consider a set of observations  
191  $\mathbf{x}_1, \dots, \mathbf{x}_n$  which is assumed to be iid observations from  $F(\mathbf{x})$ , and hence can  
192 be used to obtain an estimate of  $F(\mathbf{x})$ , termed  $\hat{F}(\mathbf{x})$ . When  $F(\mathbf{x})$  is com-  
193 pletely unspecified, the non parametric estimate  $\hat{F}(\mathbf{x}) = \frac{1}{n} \sum_{i=1}^n I(\mathbf{x}_i < \mathbf{x})$   
194 can be used. The non-parametric bootstrap algorithm is given in Algo-  
195 rithm 3, see Efron (1979). In the EnKF setting one will naturally resample  
196 the ensemble members  $[\mathbf{x}^{u(i)}; i = 1, \dots, n_e]$ . The bootstrap sampling may  
197 also be performed in a semi-parametric or parametric setting. In the EnKF  
198 setting semi-parametric bootstrapping could be centered at the traditional  
199 Kalman gain estimate  $\hat{\Gamma}_{\mathbf{x}, \mathbf{d}}(\hat{\Sigma}_{\mathbf{d}})^{-1}$ , and the deviations from this  $\hat{K}$  could  
200 be bootstrapped. The exact algorithm will be described in the next section.  
201 Parametric bootstrapping replaces  $\hat{F}(\mathbf{x})$  with a parametric model, and in the  
202 EnKF setting it is natural to bootstrap  $\mathbf{x}^u$  from  $N_{p_{\mathbf{x}}}(\hat{\boldsymbol{\mu}}_{\mathbf{x}}, \hat{\Sigma}_{\mathbf{x}})$ , where  $\hat{\boldsymbol{\mu}}_{\mathbf{x}}$  and  
203  $\hat{\Sigma}_{\mathbf{x}}$  are estimates of  $\boldsymbol{\mu}_{\mathbf{x}}$  and  $\Sigma_{\mathbf{x}}$ , respectively, based on the ensemble  $\mathbf{e}$ . Note

204 that unless  $n_e > p_{\mathbf{x}}$  the estimate  $\widehat{\Sigma}_{\mathbf{x}}$  will have reduced rank. We solve this  
 205 problem by adding a small positive number to the zero-valued eigenvalues,  
 206 which in practice entails regularization.

207 One important difference between bootstrapping and Monte Carlo simu-  
 208 lation is that the bootstrap estimate of the finite sample pdf is not asymptot-  
 209 ically correct when the number of bootstrap samples tends to infinity since  
 210 sampling is done from an approximate pdf.

## 211 5. Resampling the EnKF

212 The non-parametric EnKF resampling is performed along the lines of  
 213 Expression (19), recognizing that  $K = \Gamma_{\mathbf{x},\mathbf{d}}\Sigma_{\mathbf{d}}^{-1}$ . Hence the cdf of relevance  
 214 is  $F(\mathbf{x}^u, \mathbf{d}) = F(\mathbf{d}|\mathbf{x}^u)F(\mathbf{x}^u)$  from which the characteristics  $\Gamma_{\mathbf{x},\mathbf{d}}$  and  $\Sigma_{\mathbf{d}}$   
 215 can be determined. The associated finite sample estimators are the classical  
 216 estimators given in Expressions (11) and (12). The cdf  $F(\mathbf{x})$  is only assessable  
 217 through the ensemble members  $(\mathbf{x}^{u(1)}, \dots, \mathbf{x}^{u(n_e)})$ , and may be bootstrapped  
 218 by the nonparametric  $\widehat{F}(\mathbf{x}^u)$ , see Algorithm 3. The conditional cdf  $F(\mathbf{d}|\mathbf{x}^u)$   
 219 is defined by the likelihood model  $\nu(\mathbf{x}^u, \boldsymbol{\epsilon}^{\mathbf{d}})$  which is fully specified by the  
 220 known function  $\nu(\cdot, \cdot)$  and the known pdf of  $\boldsymbol{\epsilon}^{\mathbf{d}}$ . Consequently,  $F(\mathbf{d}|\mathbf{x}^u)$   
 221 be assessed by Monte Carlo simulation, see Algorithm 2.

222 One resample replicate of the Kalman gain  $K^*$  in Expression (19) is gen-  
 223 erated by one bootstrap sample from  $\widehat{F}(\mathbf{x}^u)$ , to obtain  $(\mathbf{x}^{u*(1)}, \dots, \mathbf{x}^{u*(n_e)})$ . For  
 224 each bootstrap sample, Monte Carlo sampling from  $F(\mathbf{d}|\mathbf{x}^{u*})$  is performed  
 225 to obtain  $[(\mathbf{x}^{u*(i)}, \mathbf{d}^{*(i,j)}); i = 1, \dots, n_e, j = 1, \dots, m]$ . Based on these realiza-  
 226 tions from  $F(\mathbf{x}^u, \mathbf{d})$  the estimates  $\widehat{\Gamma}_{\mathbf{x},\mathbf{d}}^*$  and  $\widehat{\Sigma}_{\mathbf{d}}^*$  are computed to provide one  
 227 resample replicate of the Kalman gain  $K^* = \widehat{\Gamma}_{\mathbf{x},\mathbf{d}}^*(\widehat{\Sigma}_{\mathbf{d}}^*)^{-1}$ .



228 For  $n_e \gg \min(p_{\mathbf{x}}, p_{\mathbf{d}})$  full rank of  $\widehat{\Gamma}_{\mathbf{x}, \mathbf{d}}^*$  will be ensured. Note that if  
 229  $n_e < \min(p_{\mathbf{x}}, p_{\mathbf{d}})$ , the rank of  $\widehat{\Gamma}_{\mathbf{x}, \mathbf{d}}^*$  will vary dependent on the number of  
 230 duplicates in the bootstrap sample. The number of Monte Carlo replicates  
 231 for each bootstrap sample can be chosen freely such that  $m \geq p_{\mathbf{d}}$ , hence full  
 232 rank of  $\widehat{\Sigma}_{\mathbf{d}}^*$  can be ensured.

233 The number of bootstrap replicates should be identical to the num-  
 234 ber of Kalman gain replicates required in Expression (19), i.e.  $K^{*(i)}$ ;  $i =$   
 235  $1, \dots, n_e$ . Hence one replicate for each member in the unconditioned ensem-  
 236 ble  $(\mathbf{x}^{u(1)}, \dots, \mathbf{x}^{u(n_e)})$  in order to perform the conditioning.

237 The additional computational demands from the resampling strategy are  
 238 to recompute the Kalman gain  $n_e$  times in the bootstrapping step and to  
 239 recompute the likelihood function  $m$  times in the Monte Carlo step. The  
 240 former will normally be relatively inexpensive, while the cost of the latter  
 241 depends on the actual likelihood model.

242 The procedure described above defines the non-parametric Resample EnKF  
 243 algorithm, coined ResEnKF, see Algorithm 4. The basis for ResEnKF is only  
 244 the ensemble members and the given likelihood model. No additional model  
 245 assumptions are made. The resampled Kalman gains  $K_e^{*(1)}, \dots, K_e^{*(n_e)}$  will not  
 246 be independent due to coupling through the ensemble. They will, however,  
 247 reproduce more of the variability than the single Kalman gain estimate  $\widehat{K}$   
 248 will. Consequently, the coupling will be reduced.

249 The semi-parametric EnKF resampling (ResSPEnKF) is centered at the  
 250 traditional regression line of  $\mathbf{d}$  with respect to  $\mathbf{x}$ , i.e.,  $\widehat{\Gamma}_{\mathbf{d}, \mathbf{x}} \widehat{\Sigma}_{\mathbf{x}}^{-1}$ . Define a  
 251 super ensemble  $[(\mathbf{x}^{u(i)}, \mathbf{d}^{(i,j)}); i = 1, \dots, n_e, j = 1, \dots, m]$  with observations ob-  
 252 tained from Monte Carlo simulation from  $F(\mathbf{d}|\mathbf{x})$ . Generate the associated

253 deviations ensemble  $[\Delta^{(i,j)} = \mathbf{d}^{(i,j)} - \widehat{\Gamma}_{\mathbf{d},\mathbf{x}} \widehat{\Sigma}_{\mathbf{x}}^{-1} \mathbf{x}^{u(i)}; i = 1, \dots, n_{\mathbf{e}}, j = 1, \dots, m]$ .  
254 Bootstrap  $(n_{\mathbf{e}} \times m)$  samples from the deviations ensemble and define the semi-  
255 parametric bootstrap ensemble  $[(\mathbf{x}^{u(i)}, \mathbf{d}^{*(i,j)} = \widehat{\Gamma}_{\mathbf{d},\mathbf{x}} \widehat{\Sigma}_{\mathbf{x}}^{-1} \mathbf{x}^{u(i)} + \Delta^{*(i,j)}); i =$   
256  $1, \dots, n_{\mathbf{e}}, j = 1, \dots, m]$ . From this ensemble one semi-parametric bootstrap  
257 Kalman gain  $K^*$  can be determined. The resampling must be repeated  $n_{\mathbf{e}}$   
258 times to obtain  $K^{*(i)}; i = 1, \dots, n_{\mathbf{e}}$ . Note that the  $\mathbf{x}^u$  entries are left un-  
259 changed, while the associated  $\mathbf{d}^*$  values are resampled.

260 The parametric EnKF resampling (ResPEnKF) is based on resampling  
261 of  $\mathbf{x}^u$  from  $N_{p_{\mathbf{x}}}(\hat{\mu}_{\mathbf{x}}, \widehat{\Sigma}_{\mathbf{x}})$ , were the parameters are traditional estimates of  $\mu_{\mathbf{x}}$   
262 and  $\Sigma_{\mathbf{x}}$  based on the ensemble  $\mathbf{e}$ . Simulate  $n_{\mathbf{e}}$  samples of  $\mathbf{x}^u$  and Monte  
263 Carlo simulate associated values from  $F(\mathbf{d}|\mathbf{x}^u)$  to obtain  $[(\mathbf{x}^{u*(i)}, \mathbf{d}^{*(i,j)}); i =$   
264  $1, \dots, n_{\mathbf{e}}, j = 1, \dots, m]$ . Based on this set the parametric bootstrap Kalman  
265 gain  $K^*$  can be computed. Repeat the procedure  $n_{\mathbf{e}}$  times to obtain  $K^{*(i)}; i =$   
266  $1, \dots, n_{\mathbf{e}}$ . Note that the  $\mathbf{x}^u$  entries are resampled from  $N_{p_{\mathbf{x}}}(\hat{\mu}_{\mathbf{x}}, \widehat{\Sigma}_{\mathbf{x}})$  for each  
267 Kalman gain computation. The various EnKF resampling approaches are  
268 evaluated in an empirical study in the next section.

## 269 6. Empirical study

270 In order to evaluate the impact of the various resampling strategies in  
271 EnKF, we define a Gaussian prior model and two different likelihood mod-  
272 els, one Gauss-linear and one non-linear. The Gauss-linear model with all  
273 model parameters known is analytically tractable and will act as a reference.  
274 This model is described in Myrseth & Omre (2010). The model with a nonlin-  
275 ear observation likelihood demonstrates the generality of the algorithm. We  
276 start out, however, with a simple bivariate example and evaluate a one-step  
277 update. This simple case illustrates the effect of using resampling.

---

**Algorithm 4: Non-parametric Resampled Ensemble Kalman Filter**


---

Initiate:

- $n_e =$  no. of ensemble members
- $m =$  no. of Monte Carlo replicates
- $\mathbf{x}_0^{u(i)}$ ;  $i = 1, \dots, n_e$  iid  $f(\mathbf{x}_0)$
- $\boldsymbol{\epsilon}_0^{\mathbf{d}(i)} \sim N_{p_d}(\mathbf{0}, \mathbf{I}_{p_d})$ ;  $i = 1, \dots, n_e$
- $\mathbf{d}_0^{(i)} = \nu_t(\mathbf{x}_0^{u(i)}, \boldsymbol{\epsilon}_0^{\mathbf{d}(i)})$ ;  $i = 1, \dots, n_e$
- $\mathbf{e}_0 : \{(\mathbf{x}_0^u, \mathbf{d}_0)^{(i)}; i = 1, \dots, n_e\}$

for  $t = 0$  to  $T$  do

Conditioning:

Estimate  $\hat{F}(\mathbf{x}_t^u) = \frac{1}{n} \sum_{i=1}^n I(\mathbf{x}_t^{u(i)} < \mathbf{x}_t^u)$

for  $j = 1$  to  $n_e$  do

- $\mathbf{x}_t^{u*(i)} \sim \hat{F}(\mathbf{x})$ ;  $i = 1, \dots, n_e$
- $\mathbf{G} = \mathbf{0}$
- $\mathbf{S} = \mathbf{0}$

for  $k = 1$  to  $m$  do

- $\boldsymbol{\epsilon}_t^{\mathbf{d}(i),k} \sim N_{p_d}(\mathbf{0}, \mathbf{I}_{p_d})$ ;  $i = 1, \dots, n_e$
- $\mathbf{d}_t^{(i),k} = \nu_t(\mathbf{x}_t^{u*(i)}, \boldsymbol{\epsilon}_t^{\mathbf{d}(i),k})$ ;  $i = 1, \dots, n_e$
- $\mathbf{G} = \mathbf{G} + \frac{1}{n_e - 2} \sum_{i=1}^{n_e} (\mathbf{x}_t^{u*(i)} - \hat{\boldsymbol{\mu}}_{\mathbf{x}})(\mathbf{d}_t^{(i),k} - \hat{\boldsymbol{\mu}}_{\mathbf{d}})^k$
- $\mathbf{S} = \mathbf{S} + \frac{1}{n_e - 1} \sum_{i=1}^{n_e} (\mathbf{d}_t^{(i),k} - \hat{\boldsymbol{\mu}}_{\mathbf{d}}^k)(\mathbf{d}_t^{(i),k} - \hat{\boldsymbol{\mu}}_{\mathbf{d}}^k)'$
- $\hat{\boldsymbol{\Gamma}}_{\mathbf{x},\mathbf{d}}^* = \frac{1}{m} \mathbf{G}$
- $\hat{\boldsymbol{\Sigma}}_{\mathbf{d}}^* = \frac{1}{m} \mathbf{S}$
- $\mathbf{x}_t^{c(i)} = \mathbf{x}_t^{u(i)} + \hat{\boldsymbol{\Gamma}}_{\mathbf{x},\mathbf{d}}^* (\hat{\boldsymbol{\Sigma}}_{\mathbf{d}}^*)^{-1} (\mathbf{d}_t - \mathbf{d}_t^{(i)})$

Forwarding:

- $\boldsymbol{\epsilon}_t^{\mathbf{x}(i)} \sim N_{p_x}(\mathbf{0}, \mathbf{I}_{p_x})$ ;  $i = 1, \dots, n_e$
- $\mathbf{x}_{t+1}^{u(i)} = \omega_t(\mathbf{x}_t^{c(i)}, \boldsymbol{\epsilon}_t^{\mathbf{x}(i)})$ ;  $i = 1, \dots, n_e$
- $\boldsymbol{\epsilon}_{t+1}^{\mathbf{d}(i)} \sim N_{p_d}(\mathbf{0}, \mathbf{I}_{p_d})$ ;  $i = 1, \dots, n_e$
- $\mathbf{d}_{t+1}^{(i)} = \nu_{t+1}(\mathbf{x}_{t+1}^{u(i)}, \boldsymbol{\epsilon}_{t+1}^{\mathbf{d}(i)})$ ;  $i = 1, \dots, n_e$
- $\mathbf{e}_{t+1} : \{(\mathbf{x}_{t+1}^u, \mathbf{d}_{t+1})^{(i)}; i = 1, \dots, n_e\}$

Assess

- $f(\mathbf{x}_{T+1} | \mathbf{d}_0, \dots, \mathbf{d}_T)$  from  $\mathbf{e}_{T+1}$
- 

278 *6.1. Simple bivariate example*

279 The minimalistic example consider a bivariate state variable  $\mathbf{x}^u$  with  
 280 distribution  $N_2(\boldsymbol{\mu}, \boldsymbol{\Sigma})$ , where the expectation vector  $\boldsymbol{\mu} = (1, 1)^T$  and the

281 covariance matrix  $\Sigma$  has diagonal terms  $\sigma_{11} = \sigma_{22} = 1$  and off-diagonal  
282 terms  $\sigma_{12} = \sigma_{21} = 0.37$ . The likelihood model is  $[\mathbf{d}|\mathbf{x}^u] = \mathbf{H}\mathbf{x}^u + \boldsymbol{\epsilon}_d$  with  
283  $h_{11} = h_{22} = 1$  and  $h_{12} = h_{21} = 0.5$ , while each element of the error  
284 term,  $\boldsymbol{\epsilon}_d$  is independent Gaussian with zero mean and variance 0.1. The ac-  
285 tual observations are  $\mathbf{d}^o = (-2.36, -0.79)^T$ . Consequently, the example has  
286  $n_{\mathbf{x}} = n_{\mathbf{d}} = 2$ , and we focus on the conditional state variable  $\mathbf{x}^c = [\mathbf{x}^u|\mathbf{d}^o]$   
287 with associated pdf  $f(\mathbf{x}^c)$ .

288 We assess the pdf of interest  $f(\mathbf{x}^c)$  using both the traditional EnKF,  
289 Algorithm 1, and resample ResEnKF, Algorithm 4, with a range of ensemble  
290 sizes,  $n_e = 6, \dots, 20$ . Note that for the Gauss-linear assumptions used, both  
291 algorithms are asymptotically correct when  $n_e \rightarrow \infty$ .

292 The evaluation criteria for the algorithms are: Mean Square Error (MSE),  
293 where  $\text{MSE} = \text{tr} \hat{\mathbf{E}}[(\hat{\boldsymbol{\mu}}_{\mathbf{x}^c} - \boldsymbol{\mu}_{\mathbf{x}^c})(\hat{\boldsymbol{\mu}}_{\mathbf{x}^c} - \boldsymbol{\mu}_{\mathbf{x}^c})^T]$ , and Correlation between En-  
294 semble Members (CEM) defined as  $\text{tr} \widehat{\text{Corr}}(\mathbf{x}^{c(i)}, \mathbf{x}^{c(j)})$  for  $i \neq j$ . Note that  
295 the correlation between updated ensemble members is symmetric, see Ex-  
296 pression (18), hence identical for all  $i, j = 1, \dots, n_e, i \neq j$ . These criteria are  
297 assessed by averages over 10 000 Monte Carlo simulations from the model.

298 The results from the evaluation are displayed in Figure 2. The MSE and  
299 the CEM are displayed to the left and right respectively for  $n_e = 6, \dots, 20$ .  
300 While the MSE is indeed higher for the ResEnKF, we observe that the CEM  
301 is significantly reduced compared with the traditional EnKF. An increased  
302 MSE for the ResEnKF scheme can be expected as the rank of the empiri-  
303 cally estimated covariance matrices decrease. As the ensemble size increases  
304 both the MSE and the CEM appear to converge. The convergences of both  
305 the MSE and the CEM curves are caused by both algorithms being asymp-

306 totically correct for  $n_e \rightarrow \infty$ . Note that in a sequential data assimilation  
 307 setting, the increased MSE for the ResEnKF should not be critical as this  
 308 will be corrected for at later updating steps. Introducing a large ensemble  
 309 correlation, however, would be more critical as there will be a multiplica-  
 310 tive effect at later updating steps, especially when considering static forward  
 311 models. This increased ensemble coupling can eventually lead to an ensem-  
 312 ble collapse. The consequences of sequential updating in higher-dimensional  
 313 problems will be evaluated in the next section.

### 314 6.2. Model description

315 The variables of interest are  $[\mathbf{x}_0, \dots, \mathbf{x}_{11}]$ , where  $\mathbf{x}_t \in \mathbb{R}^{100}$ ; hence  $\mathbf{x}_t$  is a  
 316 100- dimensional time series. Observations are available at  $[\mathbf{d}_0, \dots, \mathbf{d}_{10}]$ . The  
 317 current time is  $T = 10$  and the objective is the forecast  $[\mathbf{x}_{11} | \mathbf{d}_0, \dots, \mathbf{d}_{10}]$ . In  
 318 Figure 3 the reference realization of  $[\mathbf{x}_{10}, \mathbf{d}_{10}]$  is presented.

The test case is defined as follows:

$$f(\mathbf{x}_0) \sim N_{100}(\mathbf{0}, \Sigma_0^x) \quad (21)$$

$$[\mathbf{x}_{t+1} | \mathbf{x}_t] = \mathbf{A}_t \mathbf{x}_t \quad (22)$$

where the initial covariance matrix  $\Sigma_0^x$  contains elements

$$\sigma_{i,j}^x = 20 \exp(-3|i - j|/20) \quad (23)$$

319 for  $i, j = 1, \dots, 100$ . The forward model defined by  $\mathbf{A}_t$  is a linear smoother that  
 320 moves in steps of 5 from left to right for each time step. Consequently, the left  
 321 part of  $\mathbf{x}_{10}$  is smoother than the right part. The example has been inspired  
 322 by a fluid flow scenario where there is a moving front where the parameters

323 are dynamic, and static surroundings. For more detail, see Myrseth & Omre  
 324 (2010).

The likelihood models are

$$[\mathbf{d}_t|\mathbf{x}_t]_0 = H_t\mathbf{x}_t + \sqrt{20}\boldsymbol{\epsilon}_t^{\mathbf{d}} \quad (24)$$

and

$$[\mathbf{d}_t|\mathbf{x}_t]_1 = (H_t\mathbf{x}_t) \circ \exp(\sqrt{0.1}\boldsymbol{\epsilon}_t^{\mathbf{d}}) \quad (25)$$

325 where  $\boldsymbol{\epsilon}_t^{\mathbf{d}} \sim N_{10}(\mathbf{0}, \mathbf{I}_{10})$ ,  $H_t$  is time-invariant and picks 10 locations, see Fig-  
 326 ure 3 and  $\circ$  denotes a Schur product. The nonlinear likelihood contains a log  
 327 normal multiplicative error structure.

### 328 6.3. Results

329 The forecast  $[\mathbf{x}_{11}|\mathbf{d}_0, \dots, \mathbf{d}_{10}]$  will be used to measure the impact of resam-  
 330 pling. The Root Mean Square Error (RMSE) of the mean forecast will be  
 331 used to measure accuracy. The coverage will be used to measure forecast  
 332 uncertainty which captures both accuracy and precision. A 95% coverage  
 333 interval should include the solution 95% of the time. If the coverage is lower  
 334 than this then the 95% forecast interval underestimates the uncertainty. The  
 335 examples are run with the ensemble sizes  $n_e = 30$  and  $n_e = 100$  with  $m = 50$   
 336 Monte Carlo samples. An empirical 95% prediction interval is defined to be  
 337 spanned by the 28 and 96 central ensemble members for the two ensemble  
 338 sizes. We should therefore expect 87.1% and 94.1% coverage for  $n_e = 30$  and  
 339  $n_e = 100$ , respectively, see Wilks (1962).

### 340 6.4. Gauss-linear likelihood model

341 For the Gauss-linear model, the model parameters are available through  
 342 the traditional Kalman Filter, this exact solution is presented in Figure 4.

343 For the Gauss-linear model also the resampling approach as outlined in Ex-  
 344 pression (20) is available. This case is termed the exact finite sample solution,  
 345 and it captures the uncertainty due to finite size of the ensemble. The tradi-  
 346 tional EnKF algorithm, Algorithm 1, the ResEnKF, Algorithm 4, adapted to  
 347 a known linear likelihood, and the ResSPEnKF and ResPEnKF algorithms  
 348 are also run on this Gauss-linear case.

349 Figures 5 and 6 and Table 1 display the results obtained for the Gauss-  
 350 linear model. In Figures 5 and 6 the prediction  $[\mathbf{x}_{11}|\mathbf{d}_1, \dots, \mathbf{d}_{10}]$  with as-  
 351 sociated 95% prediction intervals are displayed for one run of each of the  
 352 algorithms with ensemble sizes  $n_e = 30$  and  $n_e = 100$  respectively. The  
 353 reference  $\mathbf{x}_{11}$  is also displayed. Table 1 contains statistics from 100 repeated  
 354 runs of each algorithm on the same observations.

355 Figure 4 contains the analytical solution of the Kalman Filter which is  
 356 available for this Gauss-linear model. The reduction in prediction uncer-  
 357 tainty around each observation is observed. Figures 5(a) and 6(a) present  
 358 the prediction results for the exact finite sample solutions for  $n_e = 30$  and  
 359  $n_e = 100$ , see Expression (20). Recall that the Kalman gains are resampled  
 360 using  $\mathbf{x}^u \sim N_{p_x}(\boldsymbol{\mu}, \Sigma)$  which adds uncertainty relative to the analytical so-  
 361 lution which is the limiting case as  $n_e \rightarrow \infty$ . The  $n_e = 30$  case has larger  
 362 uncertainty while the  $n_e = 100$  case is very similar to the limiting case. These  
 363 exact finite sample solutions are the reference solutions for the other ensemble  
 364 Kalman filter runs. Figures 5(b) and 6(b) contain the results for the tradi-  
 365 tional EnKF algorithm. The underestimation of the prediction intervals for  
 366  $n_e = 30$  is observed and the non-logical increase in uncertainty as  $n_e$  increases  
 367 is observed for  $n_e = 100$ . We interpret the underestimation of uncertainty

368 for  $n_e = 30$  to be caused by coupling of ensemble members due to the use of  
 369 one common estimate of the Kalman gain, as discussed in previous sections.  
 370 Note that all estimated matrices used in the conditioning have full rank in  
 371 this case, since  $n_e > n_d$ . The fact that the exact finite sample solutions,  
 372 which uses independent Kalman gains for each ensemble member, exposes  
 373 decreasing uncertainty with increasing  $n_e$ , supports our interpretation. Fig-  
 374 ures 5(c) and 6(c) contain the results from the ResEnKF algorithm which  
 375 includes full bootstrapping of the ensemble members to provide Kalman gain  
 376 variability and reduce coupling in the conditional ensembles. The prediction  
 377 intervals for ResEnKF are wider than for traditional EnKF and close to the  
 378 reference exact finite sample solutions in Figures 5(a) and 6(a). This effect  
 379 is clearly seen for  $n_e = 30$ , while the results are more similar for  $n_e = 100$ .  
 380 The results for the ResSPEnKF and ResPEnKF algorithms in Figures 5(d)  
 381 and 6(d) through 5(e) and 6(e) are similar to the ones for full bootstrapping  
 382 in ResEnKF, although the ResEnKF seems to appear with better coverage  
 383 of the prediction intervals at lower ensemble sizes.

384 The results from the Gauss-linear model case can be summarized from  
 385 Table 1 as follows: The traditional EnKF appears with better prediction  
 386 accuracy than the ResEnKF algorithm, but the latter assesses the predic-  
 387 tion uncertainty more reliably. In the traditional EnKF one uses the best  
 388 estimate of the Kalman gain on all ensemble members to improve prediction  
 389 accuracy, but this introduces coupling in the ensemble and hence underes-  
 390 timation of prediction uncertainty. In ResEnKF one resamples the Kalman  
 391 gain causing loss in prediction accuracy, but this also reduces coupling in  
 392 the ensemble and hence improves the prediction uncertainty estimates. The



393 two alternative resampling approaches appear less reliable than ResEnKF.  
 394 The parametric resampling EnKF has smaller RMSE and better coverage  
 395 for small  $n_e$ , however, but the geometry of the prediction intervals in Fig-  
 396 ure 5(e) appears with too little variability. Lastly, note that these results  
 397 are obtained on a Gauss-linear model which appears as very favorable for  
 398 the EnKF. Hence the underestimation of the prediction uncertainty should  
 399 cause concern in more complex models.

#### 400 *6.5. Nonlinear likelihood model*

401 For the nonlinear likelihood the true model parameters are analytically  
 402 intractable. However, the resampling EnKF algorithm, Algorithm 4, can  
 403 be used without the bootstrapping loop. Then the likelihood model is lin-  
 404 earized by Monte Carlo sampling based linearization around the ensemble.  
 405 Hence, local ensemble dependent linearization is performed. This approach  
 406 is termed EnKF/nonlinear likelihood. Finally, the full ResEnKF algorithm,  
 407 Algorithm 4 and the semi-parametric, ResSPEnKF, and the parametric Re-  
 408 sPEnKF, including both bootstrapping and Monte Carlo sampling can be  
 409 used.

410 Figures 7 and 8 and Table 2 display the results obtained for the Gaus-  
 411 sian prior model with nonlinear likelihood model. The layout is identical  
 412 to Figures 5 and 6, and Table 1. Figures 7(a) and 8(a) display the EnKF  
 413 solutions with local, ensemble based linearization of the likelihood model for  
 414 ensemble sizes  $n_e = 30$  and  $n_e = 100$ . The prediction uncertainties are un-  
 415 derestimated for  $n_e = 30$  and uncertainty increases with increasing  $n_e$  which  
 416 is non-intuitive. Figures 7(b) and 8(b) contain the results from the ResEnKF  
 417 algorithm with full bootstrap and Monte Carlo resampling. The prediction

418 intervals for  $n_e = 30$  appear as much more reliable than for the previous al-  
419 gorithm, while intervals for  $n_e = 100$  are fairly similar. Figures 7(c) through  
420 8(d) display the results from the semi-parametric, ResSPEnKF, and para-  
421 metric, ResPEnKF, algorithms, and they appear as less reliable than the  
422 results from the ResEnKF algorithm.

423 In Table 2 statistics for 100 repeated runs of each algorithm are sum-  
424 marized. The EnKF with local, ensemble based linearization tends to un-  
425 derestimate the prediction uncertainty. The ResEnKF algorithm has higher  
426 RMSE than the EnKF with nonlinear likelihood, but provides more reli-  
427 able estimates of the prediction intervals. The two alternative resampling  
428 approaches appear less reliable than ResEnKF.

## 429 7. Conclusion

430 The traditional EnKF is based on an ensemble representing the pdf of  
431 the variable of interest. The ensemble members are sequentially conditioned  
432 on observations and forwarded to the next time step. The conditioning to  
433 available observations is the challenging part, and in EnKF this conditioning  
434 is linearized using weights corresponding to the Kalman gain. The actual  
435 Kalman gain is estimated based on all ensemble members. Since the same  
436 Kalman gain estimate is used in all the conditioning of all ensemble mem-  
437 bers it can be shown that the members end up being coupled. Eventually  
438 this will cause the prediction intervals to be underestimated. A resampling  
439 strategy where the Kalman gain is generated from its sampling distribution  
440 is suggested. This will reduce coupling in the conditioning step.

441 The resampling EnKF, ResEnKF, algorithm is defined for a model with  
442 both prior and the likelihood being on general nonlinear form. The coupling

443 of the ensemble members is reduced by bootstrapping the Kalman gains  
444 used in the conditioning step. The computational demands of ResEnKF are  
445 larger than for EnKF, but only slightly larger. The alternative resampling  
446 schemes, ResSPEnKF and ResPEnKF are also defined. The former uses a  
447 semi-parametric model in the resampling while the latter uses a resampling  
448 from a parametric model.

449 The various algorithms are evaluated empirically. In a simple, bivariate  
450 example with one updating step, the ResEnKF algorithm is demonstrated  
451 to be clearly superior to the traditional EnKF algorithm in terms of reduc-  
452 ing the ensemble correlation. This comes at the cost of a lower prediction  
453 error compared to the traditional EnKF algorithm. A Gauss-linear model is  
454 also used and the exact finite sample prediction intervals are generated as  
455 reference. It is shown that the traditional EnKF algorithm severely under-  
456 estimates the prediction intervals for small ensemble sizes. The ResEnKF  
457 has significantly higher coverage of the prediction intervals on the expense  
458 of somewhat larger mean square error of prediction itself when compared to  
459 the EnKF. The alternative resampling schemes appear less reliable.

460 The algorithms are also evaluated on a Gaussian prior model with nonlin-  
461 ear likelihood model. The ResEnKF algorithm with bootstrapping appears  
462 as more reliable than the traditional EnKF for small ensemble sizes. Overall  
463 the ResEnKF algorithm outperformed the traditional EnKF by providing  
464 more reliable prediction intervals on the expense of slightly lower prediction  
465 accuracy. The ResEnKF algorithm requires no extra modeling and has only  
466 slightly larger computational demands than the EnKF algorithm. None of  
467 the two alternative resampling schemes seem to provide results that are more

468 reliable than the full bootstrapping algorithm ResEnKF.

## 469 **8. Acknowledgments**

470 Parts of this work has been funded by the Uncertainty in Reservoir Eval-  
471 uation (URE) initiative at NTNU.

## 472 **References**

473 Anderson, J. (2001). An ensemble adjustment ensemble Kalman filter for  
474 data assimilation. Monthly Weather Review, 127, 2741–2758.

475 Bertino, L., Evensen, G., & Wackernagel, H. (2002). Combining geostatistics  
476 and Kalman filtering for data assimilation in an estuarine system. Inverse  
477 Problems, 18(1), 1–23.

478 Burgers, G., van Leeuwen, P. J., & Evensen, G. (1998). Analysis scheme in  
479 the ensemble Kalman filter. Monthly Weather Review, 126(6), 1719–1724.

480 Efron, B. (1979). Bootstrap methods: Another look at the jackknife. The  
481 Annals of Statistics, 7(1), 1–26.

482 Efron, B. & Tibshirani, R. (1993). An Introduction to the Bootstrap. Chap-  
483 man & Hall, New York.

484 Evensen, G. (1994). Sequential data assimilation with nonlinear quasi-  
485 geostrophic model using Monte Carlo methods to forecast error statistics.  
486 Journal of Geophysical Research, 99(C5), 10,143–10,162.

487 Evensen, G. (2007). Data Assimilation; The Ensemble Kalman Filter.  
488 Springer.

489 Furrer, R. & Bengtsson, T. (2007). Estimation of high-dimensional prior  
490 and posterior covariance matrices in Kalman filter variants. Journal of  
491 Multivariate Analysis, 98(2), 227–255.

492 Hammersley, J. M. & Handscomb, D. C. (1964). Monte Carlo Methods.  
493 London & New York: Chapman & Hall.

494 Houtekamer, P. & Mitchell, H. L. (1998). Data assimilation using an ensemble  
495 Kalman filter technique. Monthly Weather Review, 126(3), 796–811.

496 Houtekamer, P., Mitchell, H. L., Pellerin, G., Buehner, M., Charron, M.,  
497 Spacek, L., & Hansen, B. (2005). Atmospheric data assimilation with an  
498 ensemble Kalman filter: Results with real observations. Monthly Weather  
499 Review, 133(3), 604–620.

500 Huber, P. J. (1981). Robust Statistics. Wiley.

501 Myrseth, I. & Omre, H. (2010). Hierarchical ensemble kalman filter. SPE  
502 Journal, 15(2), 569–580.

503 Nævdal, G., Johnsen, L. M., Aanonsen, S. I., & Vefring, E. H. (2005). Reser-  
504 voir monitoring and continuous model updating using ensemble Kalman  
505 filter. SPE Journal, 10(1), 66–74.

506 Wilks, S. S. (1962). Mathematical Statistics. Wiley.

507 **List of Figures**

508 1 Hidden Markov process . . . . . 32

509	2	Empirical evaluation of MSE and CEM, using the Traditional	
510		EnKF and Resampling EnKF schemes. . . . .	33
511	3	Reference realization: $(\mathbf{x}_{10}, \mathbf{d}_{10})$ . Observations from the linear	
512		likelihood marked by triangles. Observations from the nonlin-	
513		ear likelihood marked by circles. . . . .	34
514	4	Exact solution for the Gauss-linear model. The reference re-	
515		alization (black), predictions (solid blue) and 95% prediction	
516		intervals (hatched blue). . . . .	35
517	5	Gauss-linear model. The reference realization (black), pre-	
518		dictions (solid blue) and 95%-empirical prediction intervals	
519		(hatched blue) for one run of each of the EnKF algorithms	
520		with ensemble size $n_e = 30$ . . . . .	36
521	6	Gauss-linear model. The reference realization (black), pre-	
522		dictions (solid blue) and 95%-empirical prediction intervals	
523		(hatched blue) for one run of each of the EnKF algorithms	
524		with ensemble size $n_e = 100$ . . . . .	37
525	7	Gauss-nonlinear model. The reference realization (black), pre-	
526		dictions (solid blue) and 95%-empirical prediction intervals	
527		(hatched blue) for one run of each of the EnKF algorithm	
528		with ensemble size $n_e = 30$ . . . . .	38
529	8	Gauss-nonlinear model. The reference realization (black), pre-	
530		dictions (solid blue) and 95%-empirical prediction intervals	
531		(hatched blue) for one run of each of the EnKF algorithm	
532		with ensemble size $n_e = 100$ . . . . .	39

533 **List of Tables**

534	1	Gauss-linear model. RMSE and 95% empirical coverage for	
535		the different algorithms with a Gauss-linear likelihood model	
536		averaged over 100 runs. . . . .	40
537	2	Gauss-nonlinear model. RMSE and 95% empirical coverage	
538		for the different algorithms with a nonlinear likelihood model	
539		averaged over 100 runs. . . . .	41

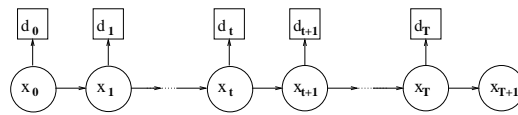
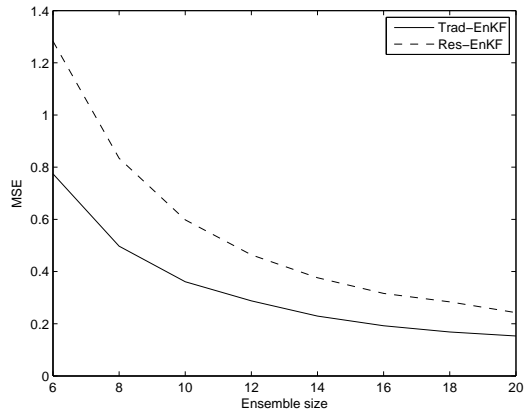
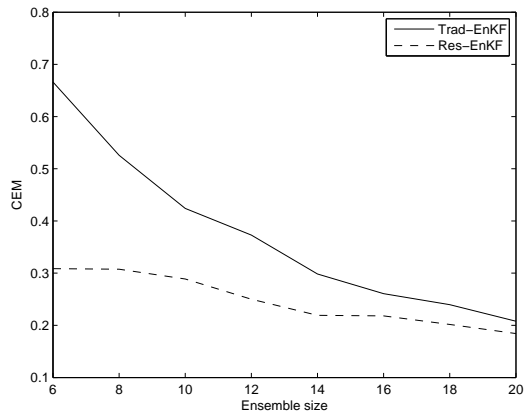


Figure 1: Hidden Markov process





(a) MSE



(b) CEM

Figure 2: Empirical evaluation of MSE and CEM, using the Traditional EnKF and Re-sampling EnKF schemes.

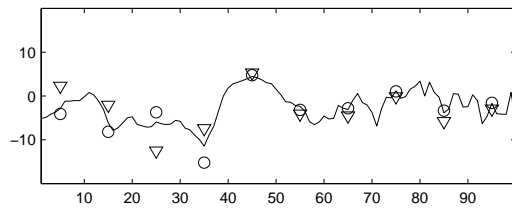


Figure 3: Reference realization:  $(\mathbf{x}_{10}, \mathbf{d}_{10})$ . Observations from the linear likelihood marked by triangles. Observations from the nonlinear likelihood marked by circles.

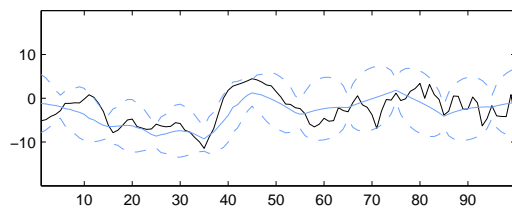


Figure 4: Exact solution for the Gauss-linear model. The reference realization (black), predictions (solid blue) and 95% prediction intervals (hatched blue).

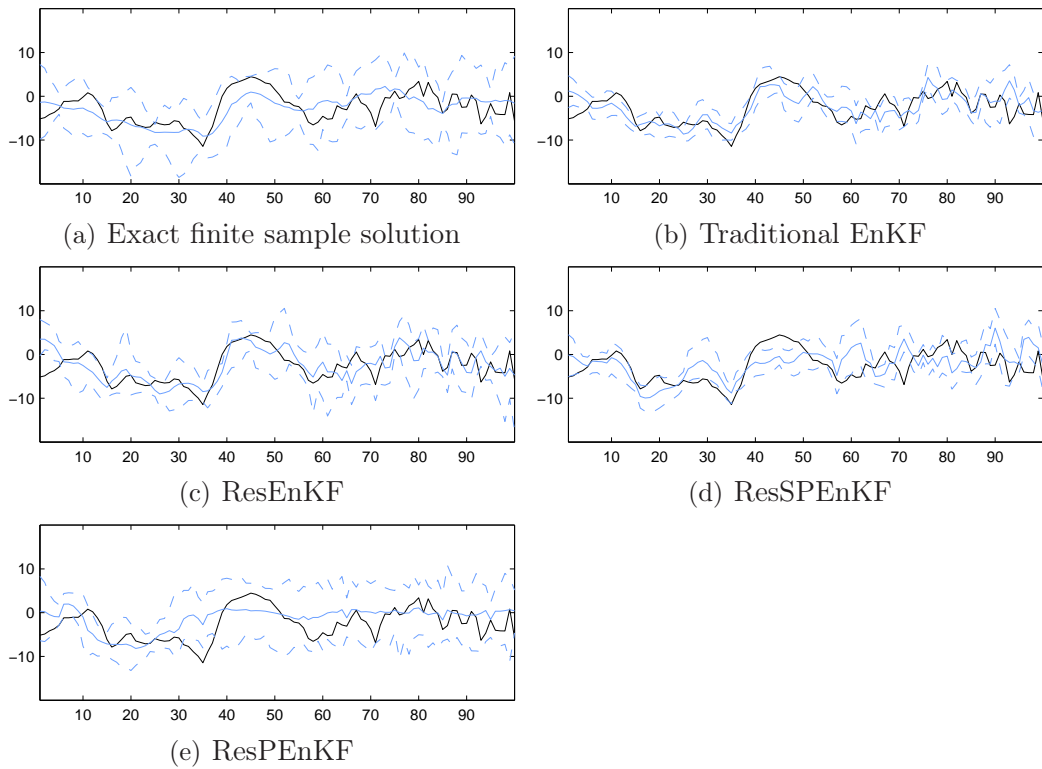


Figure 5: Gauss-linear model. The reference realization (black), predictions (solid blue) and 95%-empirical prediction intervals (hatched blue) for one run of each of the EnKF algorithms with ensemble size  $n_e = 30$ .

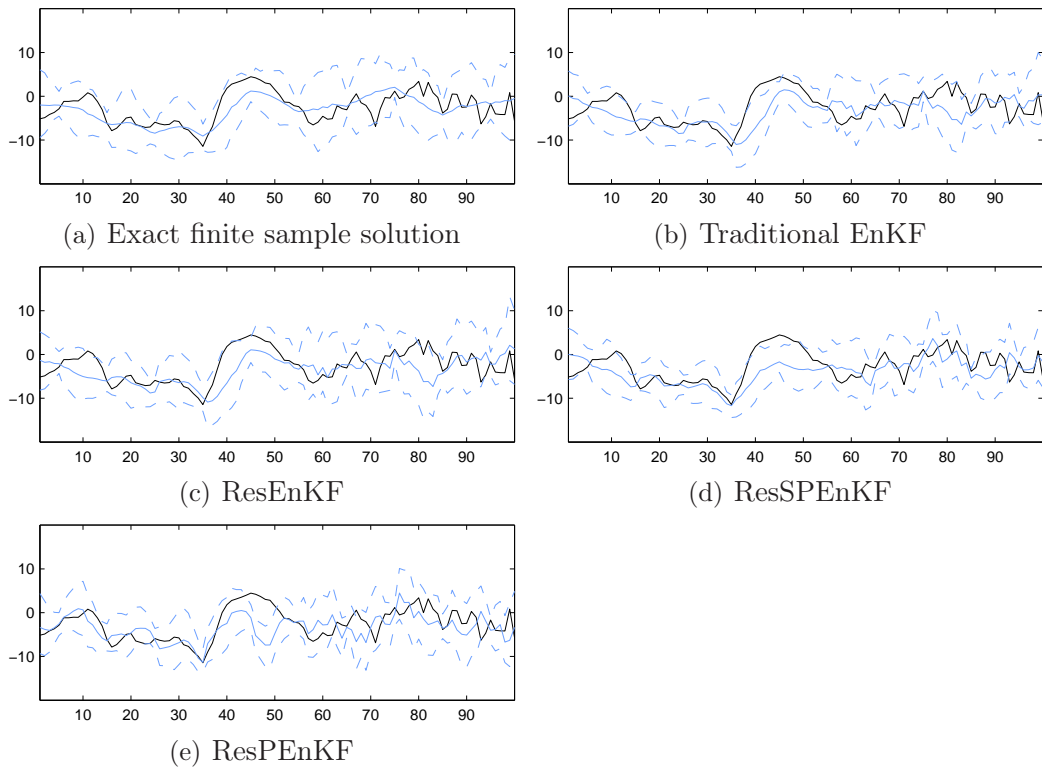


Figure 6: Gauss-linear model. The reference realization (black), predictions (solid blue) and 95%-empirical prediction intervals (hatched blue) for one run of each of the EnKF algorithms with ensemble size  $n_e = 100$ .

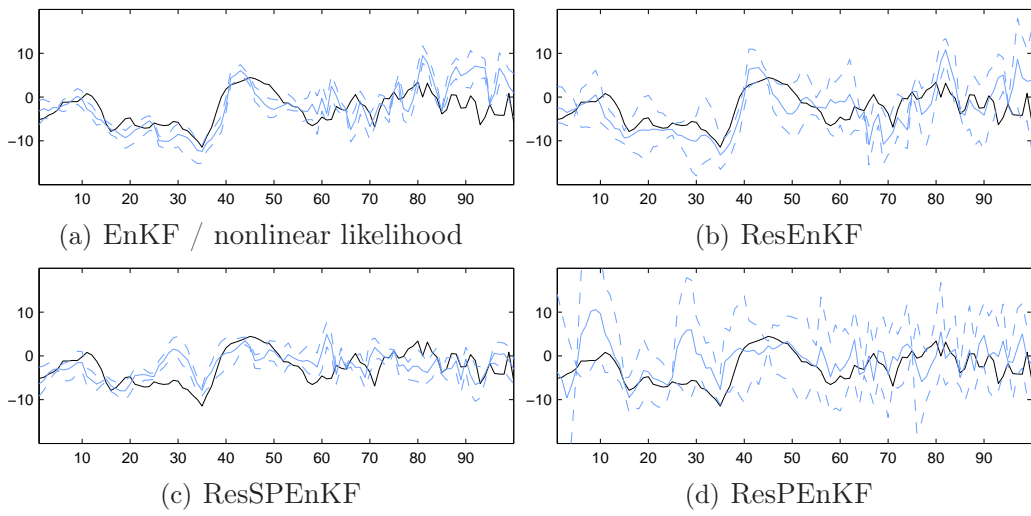


Figure 7: Gauss-nonlinear model. The reference realization (black), predictions (solid blue) and 95%-empirical prediction intervals (hatched blue) for one run of each of the EnKF algorithm with ensemble size  $n_e = 30$ .

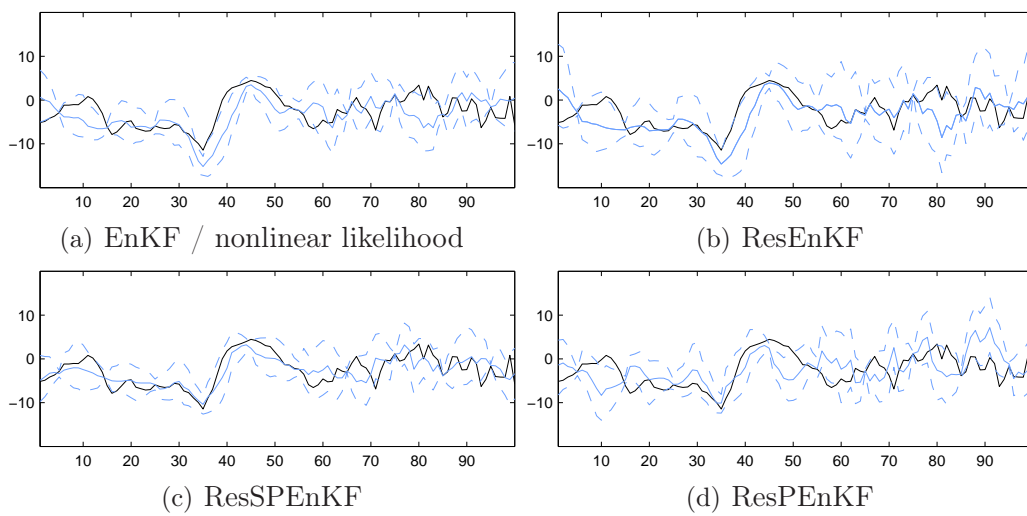


Figure 8: Gauss-nonlinear model. The reference realization (black), predictions (solid blue) and 95%-empirical prediction intervals (hatched blue) for one run of each of the EnKF algorithm with ensemble size  $n_e = 100$ .

	$n_e$	RMSE	Coverage (%)
Exact solution		2.68	95.0
Exact finite sample solution	30	2.75	97.3
Traditional EnKF	30	3.55	62.3
ResEnKF	30	3.92	74.0
ResSPEnKF	30	3.98	58.7
ResPEnKF	30	3.79	86.1
Exact finite sample solution	100	2.70	98.1
Traditional EnKF	100	2.93	88.8
ResEnKF	100	3.00	93.5
ResSPEnKF	100	3.31	83.1
ResPEnKF	100	3.52	84.8

Table 1: Gauss-linear model. RMSE and 95% empirical coverage for the different algorithms with a Gauss-linear likelihood model averaged over 100 runs.



	$n_e$	RMSE	Coverage (%)
EnKF / nonlinear likelihood	30	4.67	40.1
ResEnKF	30	5.81	67.4
ResSPEnKF	30	3.92	43.1
ResPEnKF	30	5.97	80.4
EnKF / nonlinear likelihood	100	2.95	82.0
ResEnKF	100	3.10	93.0
ResSPEnKF	100	2.93	81.3
ResPEnKF	100	3.36	82.4

Table 2: Gauss-nonlinear model. RMSE and 95% empirical coverage for the different algorithms with a nonlinear likelihood model averaged over 100 runs.